

STAR FORMATION RATE INDICATORS IN WIDE-FIELD INFRARED SURVEY Preliminary Release

Fei Shi, *Department of Basic Science, North China institute of spaceflight engineering, Hebei 065000, PR China, e-mail: fshi@bao.ac.cn*

Xu Kong, *Center of Astrophysics, University of Science and Technology of China, Jinzhai Road 96, Hefei 230026, China.*

James Wicker, *National Astronomical Observatories, Chinese Academy of Sciences, 20A Datun Road, Chaoyang District, Beijing 100012, PR China*

Yang Chen, *Center of Astrophysics, University of Science and Technology of China, Jinzhai Road 96, Hefei 230026, China.*

Zi-Qiang, Gong, *Department of Basic Science, North China institute of spaceflight engineering, Hebei 065000, PR China*

Dong-Xin, Fan, *Department of physics and Electronics, Guangxi Teachers Education University, Nanning 530001, China.*

Abstract. With the goal of investigating the degree to which the MIR luminosity in the WIDE-FIELD INFRARED SURVEY (WISE) traces the SFR, we analyze 3.4, 4.6, 12 and 22 μm data in a sample of $\sim 140,000$ star-forming galaxies or star-forming regions **covering a wide range in metallicity** $7.66 < 12 + \log(\text{O}/\text{H}) < 9.46$, **in redshift less than 0.4**. These star-forming galaxies or star-forming regions are selected by matching the WISE Preliminary Release Catalog with the star-forming galaxy Catalog in SDSS DR8 provided by JHU/MPA¹. We study the relationship between the luminosity at 3.4, 4.6, 12 and 22 μm from WISE and $\text{H}\alpha$ luminosity in SDSS DR8. From these comparisons, we derive reference SFR indicators for use in our analysis. Linear correlations between SFR and the 3.4, 4.6, 12 and 22 μm luminosity are found, and calibrations of SFRs based on $L(3.4)$, $L(4.6)$, $L(12)$ and $L(22\mu\text{m})$ are proposed. The calibrations hold for galaxies with verified spectral observations. The dispersion in the relation between 3.4, 4.6, 12 and 22 μm luminosity and SFR relates to the galaxy's properties, such as 4000Å break and galaxy color.

¹<http://www.sdss3.org/dr8/spectro/galspec.php>.

Key words: Galaxies: star formation – Galaxies: abundances – Methods: data analysis – Infrared: galaxies

1 Introduction

The star formation rate (SFR) is a crucial parameter to characterize the star formation history of galaxies. To calculate the SFR reliably, extensive efforts have been made to derive SFR indicators at various wavelengths, including radio, infrared (IR), ultraviolet (UV), optical spectral lines and continuum (Kennicutt 1998). Among these wavelengths, SFR indicators at the infrared (IR) band have attracted more attention in recent years because of the high sensitivity and high angular resolution data provided by the Spitzer Space Telescope. As a result, the general correlation between infrared luminosity and SFR has been found and calibrated (Calzetti et al. 2005, 2007, 2009, 2010, AlonsoHerrero et al. 2006, Schmitt et al. 2006, Kennicutt et al. 2007, Persic et al. 2007, Rosa et al. 2007, Salim et al. 2007, Bigiel et al. 2008, Rieke et al. 2009).

During last twenty years, the calibrations of these correlations are mainly focused on the relation between the total luminosity in the IR band (L_{TIR}) and SFR because of dust heating in the wide IR band. As a result, the monochromatic SFR indicators based on a single band measurement from galaxies are ignored to some extent. Calculation of L_{TIR} requires models for the infrared spectral energy distribution (SED) of star-forming galaxies (Chary & Elbaz 2001, Dale & Helou 2002, Lagache et al.2003, Marcillac et al.2006, Noll et al.2009), but these models usually suffer from small galaxy sample size and limited sensitivities from surveys such as Infrared Astronomical Satellite (IRAS) and Infrared Space Observatory (ISO).

Because of the shortcomings of the L_{TIR} , studies of monochromatic SFR indicators based on the single band measurement from galaxies have experienced a new resurgence, such as the emission detected in the $8\ \mu\text{m}$ and $24\ \mu\text{m}$ Spitzer bands. This emission has been analyzed by a number of authors (Calzetti et al. 2005, 2007, 2010, AlonsoHerrero et al. 2006, Perez–Gonzalez et al. 2006, Rellano et al. 2007, Salim et al. 2007, Rieke et al. 2009), but the sample size of Spitzer is small and the sensitivity is also limited.

In a word, the calibrations based on the relation between the total luminosity and SFR are still problematic because of the limitation of sensitivity and size of sample. This dearth of infrared data for normal star-forming galaxies is largely a consequence of prior instrumental limitations

The Wide-field Infrared Survey Explorer (WISE, Wright et al. 2010) will map the entire sky with $5\ \sigma$ point source sensitivities better than 0.08, 0.11, 1 and 6 mJy at wavelengths of 3.4, 4.6, 12 & $22\ \mu\text{m}$, which is 3 to 6 orders of magnitude more sensitive than previous surveys. For example, WISE is achieving 100 times better sensitivity than IRAS in the $12\ \mu\text{m}$ band. As an all-sky survey, WISE will finally return data about over 500 million objects, so it provides us a large sample of star-forming galaxies. The improved sensitivity and large sample size make it suitable for studying the evolution of galaxies.

The WISE Preliminary Release has been available to the astronomical community since April 14, 2011 and contains the attributes for 257,310,278 objects observed during the first 105 days of the survey. The data presented here were processed with initial calibrations and reduction algorithms of the WISE pipeline

derived from early survey data (Cutri et al. 2011).

This paper is organized as follows. Based on the WISE Preliminary Data Release, we present a sample to derive our SFR index calibration (Sect. 2). In Sect. 3, we study the correlation between SFR and the luminosity at 3.4, 4.6, 12 & 22 μm and calibrate the 3.4, 4.6, 12 & 22 μm SFR index. In Sect.4, we study the origin of dispersion between SFR and the luminosity at 3.4, 4.6, 12 & 22 μm . In Sect. 5, we summarize the calibration result and conclude this paper. Throughout the paper, we adopt a value of the $\Omega_M = 0.27$ and $\Omega_\Lambda = 0.73$.

2 Data sample

The preferred method for determining SFR in star-forming galaxies is obtained from the luminosity at some wavelengths. WISE is surveying the entire sky at wavelengths of 3.4, 4.6, 12 & 22 μm (**W1 through W4, respectively**), so we will study the correlation the SFR and the luminosity at 3.4, 4.6, 12 & 22 μm and calibrate them. In this paper, **the adopted SFR values are provided by JHU/MPA, determined from the method in Brinchmann et al.(2004) which combines emission line measurements from within the fiber where possible and aperture corrections are done by fitting models of Gallazzi et al (2005), Salim et al (2007) to the photometry outside the fibre. The luminosities L at 3.4, 4.6, 12 & 22 μm are calculated based on red-shift and the "raw" source flux measured in the profile-fit photometry:**

$$Flux = \frac{L}{4\pi \times D^2}$$

, where **D** is the luminosity distance derived from the red-shift.

We match the WISE Preliminary Release Catalog with the star-forming galaxy catalog in SDSS DR 8 provided by MPA. The star-forming galaxy is selected by requiring the rigorous great circle arc distances between the galaxy of SDSS and WISE Preliminary Release Catalog to be less than the 6.1'' which is the angular resolution of wavelength 1. After converting digital numbers to Jy using the PSF-fit photometry (Cutri et al. 2011), we made the internal reddening correction for the flux of all the emission lines, using the two strongest Balmer lines, $H\alpha/H\beta$ and the effective absorption curve $\tau_\lambda = \tau_V(\lambda/5500\text{\AA})^{-0.7}$, which was introduced by Charlot & Fall (2000). Then, we made use of the spectral diagnostic diagrams from Kauffmann et al. (2003) to classify galaxies as star-forming galaxies, active galactic nuclei (AGN), or unclassified. To reduce systematic and random errors, our galaxy samples are limited by the requirement that the "raw" source flux measured photometry is always larger than three times of the uncertainty in the "raw" source flux measurement in profile-fit photometry.

In total, $\sim 140,000$ star-forming galaxies are adopted in our sample.

3 Star Formation Rates Calibrator

Hydrogen recombination line fluxes have been used very extensively to estimate the SFR, since they are proportional to the number of photons produced by the hot stars, which is in turn proportional to their birthrate. Most applications of this method have been based on measurements of luminosity from the $H\alpha$ line (Kong

2004).

Star-forming regions tend to be dusty and the dust absorption cross-section peaks in the UV, and then is reprocessed by dust and emerges beyond a few μm . As a result, the luminosity at a few μm are reliable SFR indicators. This process is restricted by the complex physical conditions, such as not all of the luminous energy produced by recently formed stars is re-processed by dust in the infrared depending on dust amount and evolved non-star-forming stellar populations also heat the dust that then emits in the FIR, etc(Calzetti et al. 2010, and references therein). So it is necessary to check whether the IR luminosity can be reliable SFR indicators.

To check whether the luminosities at 3.4, 4.6, 12 & 22 μm are reliable SFR indicators, we show the relation between $\text{H}\alpha$ luminosity and the luminosity at 3.4, 4.6, 12 & 22 μm for our data sample in Fig. 1. Apart from a few outliers in the sample, all the objects merge into a relatively tight, linear, and steep sequence, which gives the strong evidence that the luminosities at 3.4, 4.6, 12 & 22 μm are good SFR indicators just like the $\text{H}\alpha$ line.

From the relation between SFR and the luminosity at 3.4, 4.6, 12 & 22 μm for our data sample in Fig. 2, we can define a new SFR calibration. The observed distribution of all the points in this figure is linear least-square-fitted by the expression given as the dashed line in Fig. 2.

It should be noted that our SFR calibration holds only for the galaxies with authentic spectral observation. Only galaxies which have reasonable values of oxygen abundance come into Fig. 2 (~70,000 galaxies). All these galaxies have

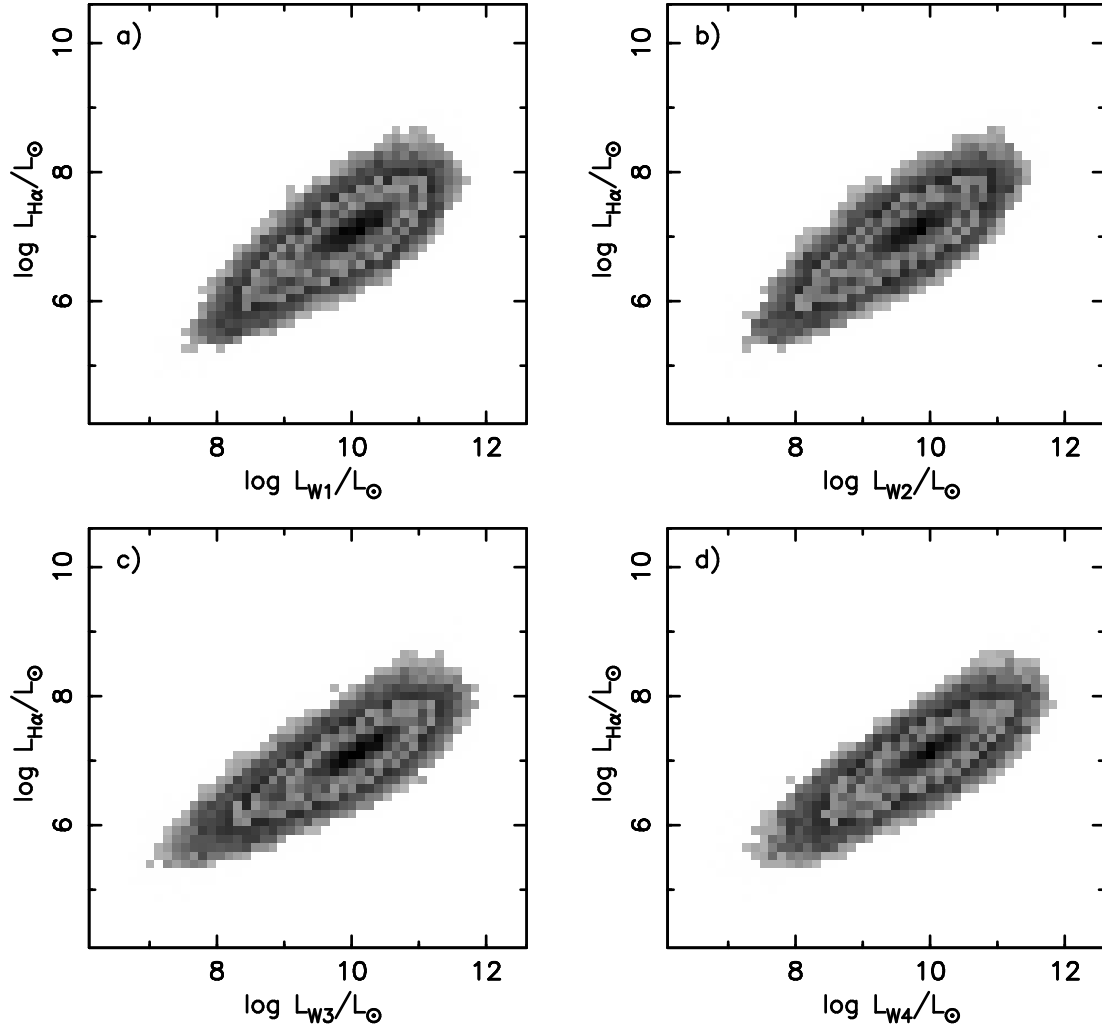


Figure 1: The relation between H α luminosity and the luminosity at W1 through W4, respectively, for our data sample. The luminosity is in units of solar luminosity.

high quality spectral observations. If we plot the whole sample into Fig. 2, the dependencies of SFR on the luminosity at 3.4, 4.6, 12 & 22 μm will worsen.

In the next section, these fit's residuals will be discussed.

4 The origin of the dispersion

This close correlation between SFR and the luminosity can be understood by the knowledge of the domination of the young star at the wavelengths of 12 & 22 μm . **The contribution from the evolved non-star-forming stellar populations at the wavelengths of 12 & 22 μm are negligible for most star-forming galaxies in our sample .** But for the wavelengths of 3.4, 4.6 μm , it is established that the contribution by the old star populations can be non-negligible in these wavelengths. The strong correlation for the wavelength of 3.4, 4.6 μm in our data sample gives strong evidence that the contribution of young stellar populations are still dominate at the wavelength of 3.4, 4.6 μm .

Although the SFR is closely related to the luminosity at 3.4, 4.6, 12 & 22 μm , the dispersion of the relation is significant. Furthermore, the scatter does not show significant change for increasing wavelength, but appears to increase for increasing luminosity (Fig. 2).

4.1 Metallicity and Concentration index

To further investigate these trends, we subdivide the sample into sub-samples with different oxygen abundances (Fig. 3a). The luminosity-SFR relation at low oxy-

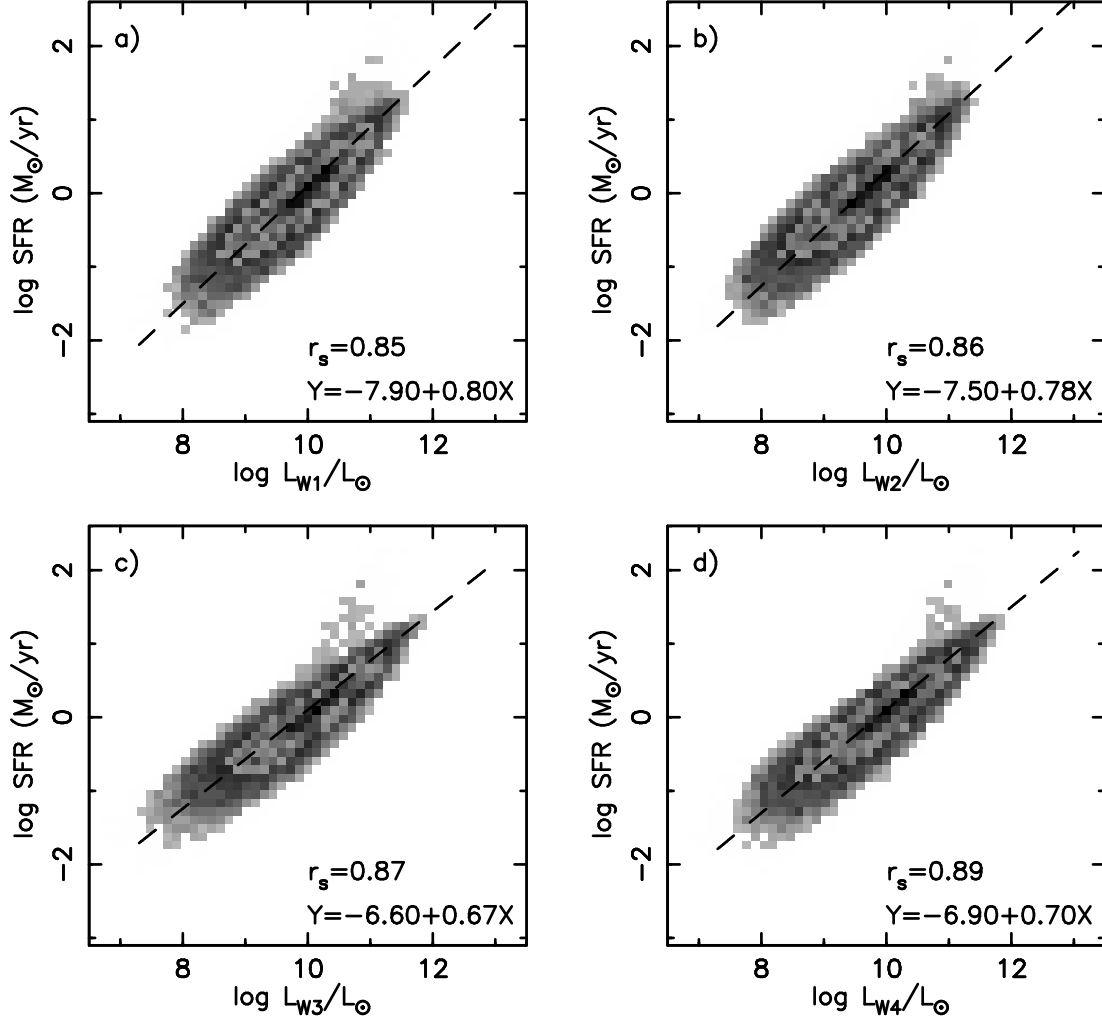


Figure 2: The relation between SFR and the luminosity at 3.4, 4.6, 12 & 22 μm for our data sample. The black lines denote the best-fit function. X and Y are luminosity and SFR, respectively. The SFR is in units of M_{sun}/yr . The luminosity is in units of solar luminosity. r_s is the standard deviation of the fit.

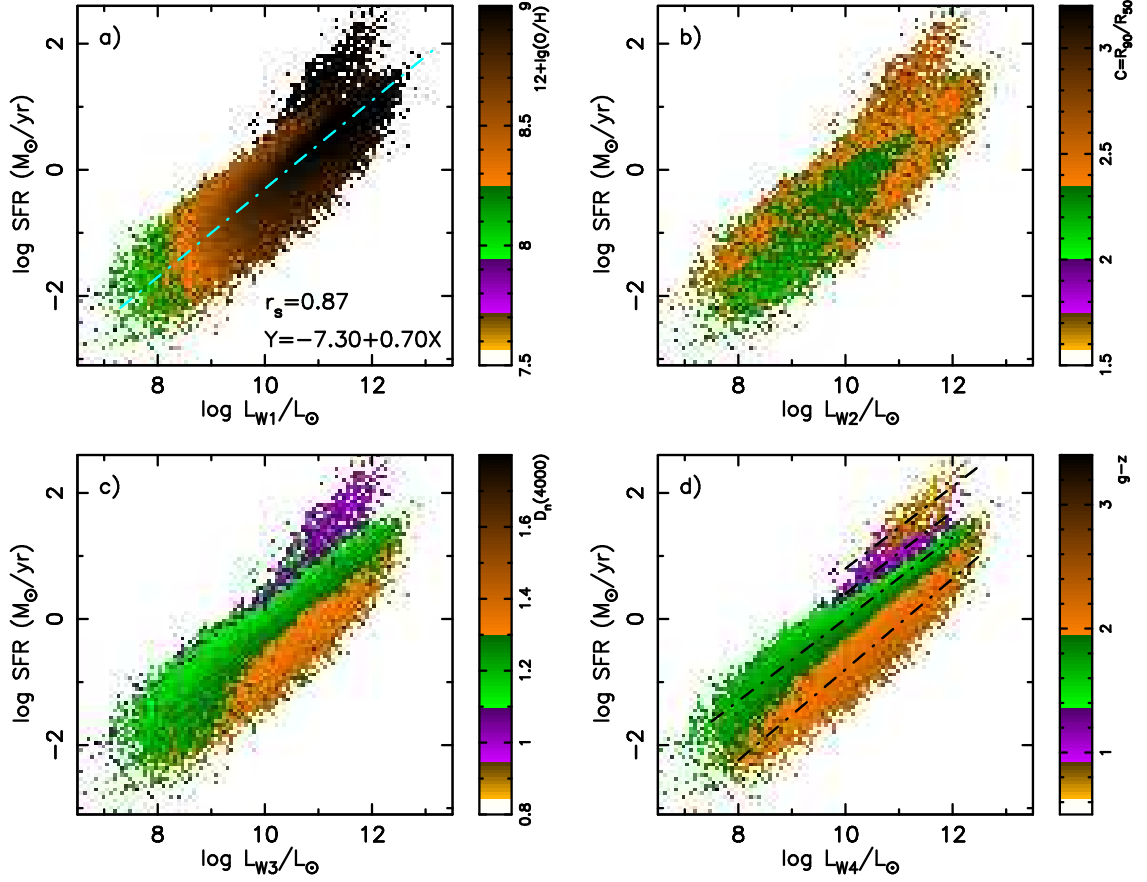


Figure 3: The relation between SFR and the luminosity for our data sample. The sample in a) is subdivided into different oxygen abundances. X and Y are luminosity and SFR, respectively. r_s is the standard deviation of the fit. The sample in b) is subdivided into different concentration values. The sample in c) is subdivided into different 4000Å breaks. The sample in d) is subdivided into different $g-z$ colors. The luminosity is in units of solar luminosity.

gen abundance is displaced to lower SFR and lower luminosity. We can explain this because the majority of low oxygen abundance galaxies have less star forming events, therefore they have relatively lower SFR.

The behavior that the higher oxygen abundance galaxies tends to have higher luminosity (mass) has been studied by many authors (Shi et al. 2005, and references therein). With the luminosity and metallicity correlation, the most straightforward interpretation is that more massive galaxies form fractionally more stars in a Hubble time (higher luminosity) than low-mass galaxies, and then have higher metallicity.

The galaxies with the concentration value $C > 2.6$ are mostly early type galaxies whereas late type galaxies have $C < 2.6$ (Kauffmann et al. 2003). It is well known that early type galaxies are dominated by old/small mass stars and late type galaxies are dominated by young/massive stars. In Fig. 3b, we subdivide the sample into sub-samples with different C . It is clear that the concentration value does not contribute to the dispersion.

4.2 4000Å break

To show the contribution of the star formation history to the dispersion in the relation between SFR and the luminosity at 3.4, 4.6, 12 & 22 μm , we divided the data sample into sub-samples with different 4000Å breaks (Fig. 3c).

We caution that because these 4000Å break quantities are derived within the fiber aperture, they may not be representative of the galaxy as a whole, whereas the SFR estimates are for the entire galaxy. **If we make the same plot using**

SFR within the fiber aperture, we still recover a similar behavior as Fig. 3c which use the SFR of the entire galaxy. From that, we can conclude that the influence of the fiber aperture effect on this relation is negligible.

It shows that the luminosity-SFR relation at a low 4000Å break is displaced to higher SFR and lower luminosity. Brinchmann et al.(2004) show that most of the star formation takes place in galaxies with a low 4000Å break. It can explain the behavior of the low 4000Å break displaced to higher SFR, where galaxies with a low 4000Å break have a younger stellar population, and therefore higher SFR values than high 4000Å break galaxies of the same SFR. The selection effects also contribute to the effect that high 4000Å break galaxies tend to be excluded from our data sample because these galaxies usually have old stellar populations and seldom show evident emission lines. If one high 4000Å break galaxy indeed shows an evident emission line, it will tend to have less starbursts, hence the lower SFR.

4.3 g-z color

It is interesting to study whether color relates to SFR or not. To show this view clearly, we divided the data sample into sub-samples with different g-z colors (Fig. 3d).

It shows that the luminosity-SFR relation at the bluer end is displaced to higher SFR and lower luminosity. We can explain this trend like the 4000Å break where the galaxies with bluer colors are younger, and therefore have a lower 4000Å break. The observed distribution of the points in each g-z color bin is linear least-

square-fitted by the following expression, given as the dashed line in Fig. 3d.

$$\lg(SFR) = -5.70 + 0.65 \lg(L_{W4}) \quad (g - z \leq 0.95) \quad (1)$$

$$\lg(SFR) = -6.10 + 0.65 \lg(L_{W4}) \quad (0.95 < g - z \leq 1.35) \quad (2)$$

$$\lg(SFR) = -6.50 + 0.65 \lg(L_{W4}) \quad (1.35 < g - z \leq 1.95) \quad (3)$$

$$\lg(SFR) = -8.00 + 0.72 \lg(L_{W4}) \quad (g - z > 1.95) \quad (4)$$

5 Conclusions

We have collected from WIDE-FIELD INFRARED SURVEY (WISE), a large sample of star-forming galaxies covering a wide range in metallicity $7.66 < 12 + \log(\text{O}/\text{H}) < 9.46$, in redshift less than 0.4, and matched the data with a sample of SDSS DR8 data. We have found the existence of the correlation between 3.4, 4.6, 12 and $22 \mu\text{m}$ luminosity and SFR and have obtained a calibration that can be used as a method for determining SFR for star-forming galaxies. The calibrations hold for galaxies with high quality spectral observations. The dispersion and non-linearity between 3.4, 4.6, 12 and $22 \mu\text{m}$ luminosity and SFR is related to the galaxy's properties, such as the 4000\AA break and galaxy color.

6 acknowledgements

This work was funded by the National Natural Science Foundation of China (NSFC) (Grant No. 10873012), the National Basic Research Program of China (973 Program) (Grant No. 2007CB815404), the Chinese Universities Scientific Fund (CUSF), and the Special fund for Ph.D of North China Institute of Aerospace Engineering(KY-2010-02-B).

This publication makes use of data products from the Wide-field Infrared Survey Explorer, which is a joint project of the University of California, Los Angeles, and the Jet Propulsion Laboratory/California Institute of Technology, funded by the National Aeronautics and Space Administration. Funding for the Sloan Digital Sky Survey (SDSS) has been provided by the Alfred P. Sloan Foundation, the Participating Institutions, the National Aeronautics and Space Administration, the National Science Foundation, the U.S. Department of Energy, the Japanese Monbukagakusho, and the Max Planck Society.

References

- [1] Alonso-Herrero, A., Rieke, G.H., Rieke, M.J., Colina, L., Perez-Gonzalez, P.G., & Ryder, S.D. 2006, ApJ, 650, 835
- [2] Balogh, M. L., Schade, D., Morris, S. L., Yee, H. K. C., Carlberg, R. G., & Ellingson, E. 1998, ApJL, 504, L75

- [3] Bigiel, F., Leroy, A., Walter, F., Brinks, E., de Blok, W.J.G., Madore, B., Thornley, M.D. 2008, AJ, 136, 2846
- [4] Brinchmann, J., Charlot, S., White, S. D. M., Tremonti, C., Kauffmann, G., Heckman, T., & Brinkmann, J. 2004, MNRAS, 351, 1151
- [5] Calzetti, D., Kennicutt, R.C., Bianchi, L., Thilker, D.A., Dale, D.A., Engelbracht, C.W., Leitherer, C., Meyer, M.J., et al. 2005, ApJ, 633, 871
- [6] Calzetti, D., Kennicutt, R. C., Engelbracht, C. W., et al. 2007, ApJ, 666, 870
- [7] Calzetti, D., & Kennicutt, R. C. 2009, PASP, 121, 937
- [8] Calzetti, D., et al. 2010, ApJ, 714, 1256
- [9] Charlot, S, Fall, S. M. 2000, ApJ, 539, 718C
- [10] Chary, R., & Elbaz, D. 2001, ApJ, 556, 562
- [11] Cutri, R. M., et al. 2011, Explanatory Supplement to the WISE Preliminary Data Release Products, 1
- [12] Dale, D. A., & Helou, G. 2002, ApJ, 576, 159
- [13] Gallazzi, A., Charlot, S., Brinchmann, J., White, S. D. M., & Tremonti, C. A. 2005, MNRAS, 362, 41
- [14] Kauffmann, G., et al. 2003, MNRAS, 346, 1055
- [15] Kennicutt, R. C. 1998, ARA&A, 36, 189

- [16] Kennicutt, R.C., Calzetti, D., Walter, F., Helou, G.,m Hollenbach, D., Armus, L., Bendo, G., Dale, D.A., Draine, B.T., Engelbracht, C.W., et al. 2007a, *ApJ*, 671, 333
- [Kong(2004)] Kong, X. 2004, *A&A*, 425, 417
- [17] Lagache, G., Dole, H., & Puget, J.-L. 2003, *MNRAS*, 338, 555
- [18] Mann, R. G., et al. 2002, *MNRAS*, 332, 549
- [19] Marcillac, D., Elbaz, D., Chary, R. R., Dickinson, M., Galliano, F., & Morrison, G. 2006, *A&A*, 451, 57
- [20] Noll, S., Burgarella, D., Giovannoli, E., Buat, V., Marcillac, D., & Muñoz-Mateos, J. C. 2009, *A&A*, 507, 1793
- [21] Perez-Gonzalez, P.G., Kennicutt, R.C., Gordon, K.D., Misselt, K.A., Gil de Paz, A., Engelbracht, C.W., Rieke, G.H., Bendo, G.J., Bianchi, L., Boissier, S., Calzetti, D., Dale, D.A., et al. 2006, *ApJ*, 648, 987
- [22] Persic, M., & Rephaeli, Y. 2007, *A&A*, 463, 481
- [23] Pilyugin, L. S., Contini, T., & Vílchez, J. M. 2004, *A&A*, 423, 427
- [24] Relaño, M., Lisenfeld, U., Perez-Gonzalez, P.G., Vilchez, J.M., & Battaner, E. 2007, *ApJ*, 667, L141
- [25] Rieke, G. H., Alonso-Herrero, A., Weiner, B. J., Pérez-González, P. G., Blaylock, M., Donley, J. L., & Marcillac, D. 2009, *ApJ*, 692, 556

- [26] Rosa–Gonzalez, D., Burgarella, D., Nandra, K., Kunth, D., Terlevich, E., & Terlevich, R. 2007, *MNRAS*, 379, 357
- [27] Schmitt, H.R., Calzetti, D., Armus, L., Giavalisco, M., Heckman, T.M., Kennicutt, R.C., Leitherer, C., & Meurer, G.R. 2006, *ApJS*, 164, 52
- [28] Salim, S., et al. 2007, *ApJS*, 173, 267
- [29] Shi, F., Kong, X., Li, C., & Cheng, F. Z. 2005, *A&A*, 437, 849
- [30] Stanghellini, L., García-Lario, P., García-Hernández, D. A., Perea-Calderón, J. V., Davies, J. E., Manchado, A., Villaver, E., & Shaw, R. A. 2007, *ApJ*, 671, 1669
- [31] Wright, E. L., et al. 2010, *AJ*, 140, 1868
- [32] Zheng, X. Z., Dole, H., Bell, E. F., Le Floch, E., Rieke, G. H., Rix, H.-W., & Schiminovich, D. 2007, *ApJ*, 670, 301
- [33] Zhu, Y.-N., Wu, H., Cao, C., & Li, H.-N. 2008, *ApJ*, 686, 155